

# 行政院國家科學委員會專題研究計畫 期中進度報告

## 多孔性球型燃燒器火燄及流場穩定性實驗與數值分析(1/2)

計畫類別：個別型計畫

計畫編號：NSC93-2212-E-009-011-

執行期間：93年08月01日至94年07月31日

執行單位：國立交通大學機械工程學系(所)

計畫主持人：陳俊勳

報告類型：精簡報告

處理方式：本計畫可公開查詢

中 華 民 國 94 年 6 月 20 日

# THE FLAME TRANSITION ANALYSES FOR METHANE-NITROGEN FUELS OVER A TSUJI BURNER

Da-Da Chen, Yao-Ching Tsai and Chiun-Hsun Chen

Department of Mechanical Engineering  
National Chiao Tung University, HsinChu 30056, Taiwan

## Abstract

This study investigates the relationship between the flame transition and the diluted percentage of nitrogen in the methane/nitrogen mixture. Both numerical and experimental works find that in the regime of  $Y_{CH_4} \leq 0.6$ , the envelope flame will transform into wake one directly when incoming velocity gradually increases to a limiting value. On the other hand, in the regime of  $Y_{CH_4} > 0.6$ , the lift-off flame, which is only survived for a moment in the experiment, or extinction will appear between the envelop and wake ones as the velocity increases. From the numerical results, it is identified that the envelope flame is a pure diffusion one, whereas the wake flame shows the characteristics of a premixed flame in the reaction front region. As to the lift-off flame, this study finds that the fuel and oxidizer is incompletely mixed and it lacks a recirculation flow to re-ignite the flammable mixture, leading to extinction. Besides, this study also finds that the flame transition limit is reduced as the mass fraction of methane in fuel mixture is lowered. The predicted trend is similar to the one observed experimentally.

## 1 Introduction

This work experimentally and numerically studies the flame behaviours over a Tsuji burner, from which methane/nitrogen mixture is ejected from the forward half part with  $v_w = 5\text{cm/s}$  into the incoming air flow. It aims to better understand the relationship among the flame transition, dilution percentage of nitrogen in the methane/nitrogen mixture and incoming flow velocity.

Tsuji and Yamaoka [4, 5, and 6] and Tsuji [7] conducted a series of experiments on the counterflow diffusion flame in the forward stagnation region of a porous cylinder. They identified two flame extinction limits. The blow-off, caused by a large velocity gradient (flame stretch), occurs because of chemical limits on the combustion rate in the flame zone. Additionally, Tsuji and Yamaoka [8] found that the dilution effect of nitrogen may influence extinction limits. However, no lift-off flame phenomenon was reported.

The combustion model developed by Chen and Weng [1] simulated the stabilization and extinction of a flame over a porous cylindrical burner. Their model employs two dimensional, complete Navier-Stokes momentum, energy, and species equations with one-step finite-rate chemical kinetics. They identified that the envelope, side, and wake flames appear in order as the incoming flow velocity is gradually increased. When a limiting value is reached, the flame is completely blown-off from the porous cylinder without any appearance of lift-off flame. However, such prediction contradicts to the experimental observations by Tsa et al. [3]. These possible reasons may contribute to the unsuitable assumptions made by that model, such as the fixed

temperature distribution along the cylinder surface, the one-step overall chemical kinetics in gas phase and so on.

In this work, the combustion model modifies Chen and Weng's one [1] by using the appropriate boundary conditions along the burner surface and the experimental set-up adds a gas mixer to the apparatus of Tsa et al. [3]. The parametric studies are given by changing the inflow velocity and the dilution percentage of nitrogen in the methane/nitrogen mixture, respectively. The predicted results are compared with the corresponding ones observed by the experiments in order to understand the physical mechanism for the flame transition over a Tsuji burner.

## 2 Experimental Apparatus and Operation Procedure

### 2.1 Experimental Apparatus

Basically, the present experimental apparatus is same as that in Tsa et al. [3], except a gas mixer is added to generate desired methane-nitrogen mixture. The experimental setup consists of three major elements, which are the wind tunnel, gas mixer and Tsuji burner. Its schematic configuration is shown in Fig. 1.

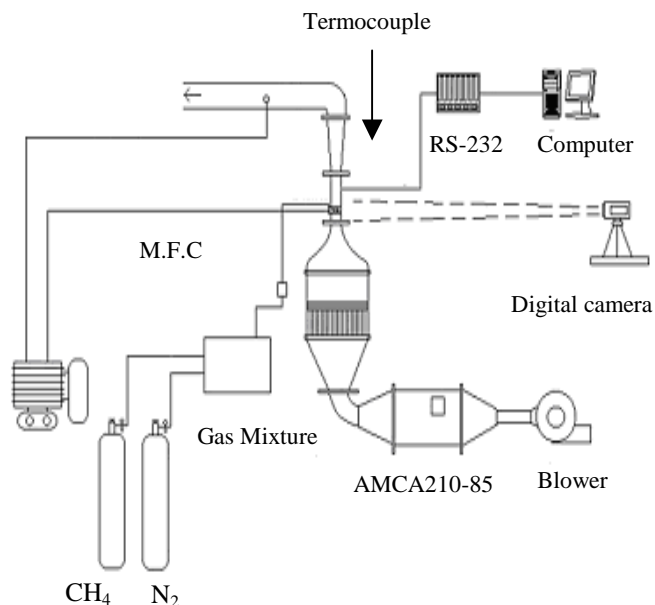


Figure 1 Schematic drawing of overall experimental system

The wind tunnel is designed to provide a laminar, uniform oxidizer flow to the porous cylindrical burner. It is open-circuit and orientated vertically upwards.

The porous cylindrical burner is comprised of inner and outer parts. The diameter of the inner part is  $20\pm 0.5$  mm, and that of outer part is  $30\pm 0.5$  mm. The inner part is a cylindrical brass rod with internal water-cooling and fuel supply grooves. The outer part is made of porous sintered stainless steel ( $20\mu\text{m}$  pores), and it is a replaceable piece with a length of  $40\pm 0.5$  mm. The outer part is screwed onto the inner one.

The function of gas mixer is to mix the methane with nitrogen well in an assigned concentration.

## 2.2 Operation Procedure

In the experiment, as shown in Fig. 1, fuel, supplied from a gas mixer, goes through the Tsuji burner and is ejected from its forward half part at a fixed velocity of  $v_w = 5\text{cm/s}$ . For safety reason, the ignition is taken at lower inflow speed to generate a flame, then, it is increased to the assigned flow velocity. The main purpose of this action is to obtain an enveloped stable flame initially. It is worth noting that the ignition device should be operated before the fuel supply valve is open; otherwise it may cause an explosion. Then, the ignition device is removed to avoid the interference with inflow. Eventually, the blower is adjusted to generate a desired flow velocity, and the resultant flame configurations are observed from the frontage of test section and recorded by a digital video camera in the whole process.

Performing this experiment, it is found that the flame transition limits will be larger if we don't measure them until the front and back walls of the test section are cooled completely. The discrepancy can be up to 0.3 m/s. Besides, between 6~18 seconds after ignition, the discrepancy is found to be about 0.2 m/s per 6 seconds. This is because that the incoming flow has been preheated in advance. As a consequence, the flame transitions will be delayed. This phenomenon was explained by Jiang et al. [2]. Although, we have measured the flame transition limits individually, the transient time from the ignition to the desired incoming velocity will take approximately 6~9 seconds. Hence, the preheated effect can not be avoided.

## 3 Mathematical Model

The combustion model adopts the following assumptions. They are: the fluid is with constant and equal specific heats, equal diffusion coefficients, and constant Prandtl and Lewis numbers for all species. The reactants and products obey the ideal gas law. The flow is steady, two-dimensional, and laminar. The gas-phase radiation, viscous dissipation and compression work are negligible and the gas phase chemistry is described by a one-step overall chemical reaction, in which frequency factor, activation energy and heat of reaction are  $1.58\cdot 10^9\text{m}^3/\text{Kg}\cdot\text{s}$ ,  $1.35\cdot 10^5\text{KJ}/\text{Kg}\cdot\text{mole}$  and  $4.95\cdot 10^4\text{KJ}/\text{Kg}\cdot\text{fuel}$ , respectively. The normalization procedure and the corresponding solution methodology, including a grid generation technique and algorithm, are similar to those developed by Chen and Weng [1]. The major improvements involve the energy coupling and the mass balance for methane/nitrogen mixture at interface between the gas and solid phases. They are described as follow.

Along the blowing surface of cylindrical burner:

$$v_t = 0, v_n = \text{assigned value}, \mathbf{n}\hat{\mathbf{x}}_w = v_n \rho_w$$

$$\mathbf{n}\hat{\mathbf{x}}_w (T_w - T_a) = \frac{1}{\text{Re Pr}} \mu \frac{\partial T}{\partial n} \Big|_w - \frac{T_w^3}{\rho^* C_p \mu_{in}} \bar{\sigma} \epsilon_w (T_w^4 - T_a^4) - \frac{\rho_{water}}{\rho^* C_p} C_{p,water} V_{water} (T_w - T_{water})$$

$$\mathbf{n}\hat{\mathbf{x}}_w (Y_{CH_4} - Y_{CH_4}) = \frac{1}{\text{Re Pr Le}} \mu \frac{\partial Y_{CH_4}}{\partial n} \Big|_w$$

$$\mathbf{n}\hat{\mathbf{x}}_w Y_{O_2} = \frac{1}{\text{Re Pr Le}} \mu \frac{\partial Y_{O_2}}{\partial n} \Big|_w$$

Along the nonblowing surface of cylindrical burner:

$$v_t = 0, v_n = 0$$

$$\frac{1}{\text{Re Pr}} \mu \frac{\partial T}{\partial n} \Big|_w = \frac{T_w^3}{\rho^* C_p \mu_{in}} \bar{\sigma} \epsilon_w (T_w^4 - T_a^4) + \frac{\rho_{water}}{\rho^* C_p} C_{p,water} V_{water} (T_w - T_{water})$$

$$\frac{\partial Y_{CH_4}}{\partial n} \Big|_w = 0, \frac{\partial Y_{O_2}}{\partial n} \Big|_w = 0$$

The computational domain is two dimensional that the length and width are the same as those in the test section. In other word, the cross-stream effect is neglected. The cell number of  $218 \times 115$  points is adopted. This computational procedure is similar to that in experiments. The original guessed values are given at the envelope flame state in a lower inflow velocity regime. Then, the inflow velocity is adjusted to the assigned value to carry out the computation until the converged solutions are obtained. The computation will take approximately 1 hour to yield a converged solution.

## 4 Results and Discussion

This study compares the numerical predictions with the observed values in experiment to examine the reliability of the numerical combustion model at first. Then, it analyses the flame structures obtained from the simulations to implement the experimental observation. The corresponding results and discussion are given as follow.

### 4.1 Comparison between Experimental Observations and Predictions

The variation parameters are the inflow velocity,  $U_{in}$ , and the methane mass fractions,  $Y_{CH_4}$ , in the methane/nitrogen mixtures under a fixed blowing velocity,  $v_w = 0.05\text{m/s}$ . Fig. 2 depicts the resultant flame structures as functions of  $U_{in}$ , and  $Y_{CH_4}$ . Three flame structures are identified and they are envelop, wake and transition flames respectively. The corresponding photographs for those flame appearances will be given later. The transition flames, existed in a narrow gap between envelop and wake flame regimes, show the lift-off flame appearance or extinction. In other words, the transition flame basically is an unstable one.

In this figure, both the experimental observed values (solid line) and numerical predictions (dash line) are plotted together and they are found to have the same qualitative trend. From the quantity point of view, it can be found that the transition gap between envelop and wake flame does not exist when  $Y_{CH_4}$  is less than 0.6 for both experiment and simulation.

In other words, the envelop flame is directly transformed into wake one as the critical velocity is reached in that regime. However, the demarcation lines and the gaps between envelop and wake flames obtained from experiments appear to be higher. The major reason for this discrepancy may mainly attribute to the preheating effect of incoming flow, which let

flame become stronger, in experiment mentioned previously, although the model adopts the one-step overall chemical kinetics. Of course, the uncertainty of velocity provided by blower and three-dimensional effect may also contribute to the discrepancy. Also, this study finds that the predicted transition region, existed as the methane mass fraction ( $Y_{CH_4}$ ) greater than 0.6, has a smaller gap than the one measured experimentally. This main reason may attribute to that this study cannot take more meticulous measurements due to the fixed but not continuous graduation in the control of blower frequency. In other words, the transition velocity in experiment may be over specified.

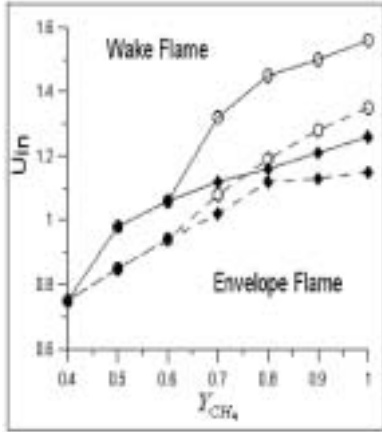


Figure 2. Flame transition limit curves for the numerical predictions and the experimental observations.

Now, this study starts to discuss the general aspects for the obtained results. From Fig. 2, it can be seen that the transition velocity is reduced as the mass fraction of methane in fuel mixture is lowered. Besides, in the lower methane mass fraction regime, ( $Y_{CH_4} \leq 0.6$ ), the envelope flame is directly transformed into wake one as the transition velocity is reached. On the other hand, in the higher methane mass fraction regime, ( $Y_{CH_4} > 0.6$ ), a transition zone existing between envelop and wake flame regimes is identified. In such zone, the flame shows oscillatory feature, in other words, it is highly unstable in experiments that it can be lift-off flame, wake flame or extinction. Whenever the lift-off flame appears, it can only sustain for less than 5 sec., then it disappears. However, it either shows a stable lift-off flame or becomes extinction by a slight increment of inflow velocity in numerical simulation.

By comparing numerical predictions with experimental observations, it can show that the combustion model can well predict the flame transition limits and simulate the envelope and wake flame structure. However, for the lift-off flame, this model can only offer the corresponding flame structure simulation and phenomenon analyses. As to the detailed transient behaviours, it needs to develop a transient program to investigate them further, which will be carried out in the near future.

#### 4.2 Flame Structure Analyses

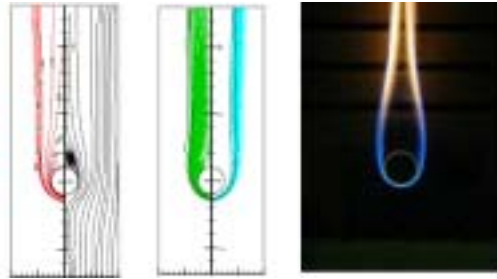
Figs.3, 4 and 5 are used to illustrate the structures of envelop, lift-off and wake flames for 100% methane in fuel (no nitrogen). In each figure, (A) is the combinations of isotherm and streamline distributions, represented by the red and black lines, respectively. (B) presents the combinations of fuel and oxidizer mass fraction and reaction rate distributions, in which green lines represent the former distribution and cyan

lines represent the oxidizer one. Also, this study adopts the  $\bar{\omega}_{CH_4} = 10^{-4} \frac{g}{cm^3 \cdot sec}$  contour line as the flame boundary,

marked by the black line. (C) is the corresponding experimental photographs to illustrate each type of flame obtained from the simulations. Remind that the velocity cannot be exactly the same for both experiment and simulation and the reasons are given previously.

##### 4.2.1 Envelope Flame

An envelope flame surrounds the porous cylinder in the low-speed inflow region, whose velocity is under 1.15m/sec. The flame structure is shown in Fig. 3. The interaction between the inflow flow and cylinder geometry make fluid flow near the cylinder decelerated and deflected. Besides, the volumetric expansion of burned gases will lead a recirculation flow to be generated behind the cylinder. The predicted flame structures are shown in Fig. 3(A) and 3(B). From Fig. 3(B), it can be seen that such flame is a diffusion flame, whose the fuel side can be distinguished from the oxidizer one. Fig. 3(C) is the experimental photograph.

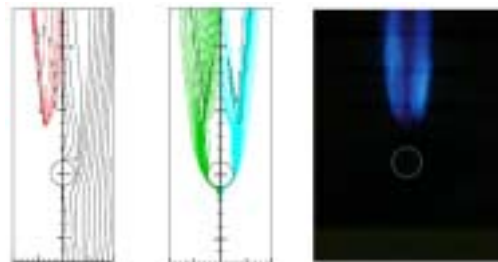


(A)  $U_{in}=0.8m/s$  (B)  $U_{in}=0.8m/s$  (C)  $U_{in}=0.8m/s$

Figure 3 Envelope flame structure

##### 4.2.2 Lift-off Flame

From numerical simulations, the study finds that the flame front will lift off from the porous cylinder when inflow velocity is further increased up to 1.16 m/sec~1.25 m/sec. It is categorized as lift-off flame. The corresponding flame structure is shown in Fig. 4. In Fig. 4(A), the volumetric expansion effect behind the cylindrical burner disappears because the flame front leaves far from the burner surface. Hence, no recirculation flow occurs behind the cylindrical burner. Therefore, the local mixing in flame front only can depend on the velocity shear and diffusion. It is expected that the fuel and oxidizer are mixed at the flame front but not well as shown in Fig. 4(B). Fig. 4(C) is the experimental photograph for lift-off flame at  $U_{in}=1.29m/s$ . Note that the velocity in Fig. 4(C) is different from the one in Fig. 4(A) and 4(B) because the transition velocities from envelope flame to transition one are not exactly the same for both experiment and simulation, mentioned previously.

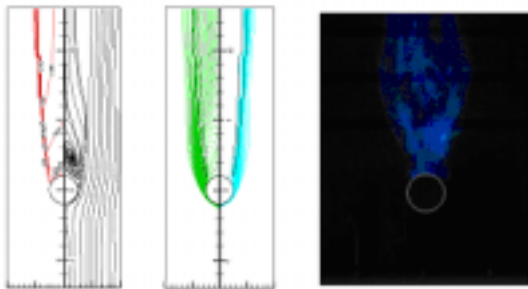


(A)  $U_{in}=1.16m/s$  (B)  $U_{in}=1.16m/s$  (C)  $U_{in}=1.29m/s$

Figure 4. Lift-off flame structure

### 4.2.3 Wake Flame

From numerical simulations, the flame front will always be situated at the rear part of the cylindrical burner when  $U_{in}$  exceeds 1.35 m/s. The flame structure is shown in Fig. 5. Fig. 5(A) shows that the recirculation flow reappears behind the cylindrical burner due to the flame situated at the rear surface of the cylindrical burner again. The recirculation flow not only brings hot gases from downstream to upstream to ignite the mixture but also stabilizes the flame. This behaviour resembles that of the bluff-body flame holder in afterburner and ramjet systems. Hence, the flames are stable again. From Fig. 5(B), this study finds the wake flame front is nearly premixed one in the front top of the reaction region. Fig. 5(C) is the experimental photograph for wake flame. As mentioned previously, the transition velocity from transition flame to stable wake one obtained from experiment is higher than prediction. Hence, the velocity in Fig. 5(A) and 5(B) is not exactly the same as that in Fig. 5(C).



(A)  $U_{in}=1.35\text{m/s}$  (B)  $U_{in}=1.35\text{m/s}$  (C)  $U_{in}=1.55\text{m/s}$

Figure 5. Wake flame structure

## 5 Conclusions

From this study, it is found that the balance between the local flow velocity and the flame speed governs the position of the flame front. As soon as the inflow velocity exceeds a limiting value, the flame front must retreat downstream to a new stable position. The transition velocity is reduced as the mass fraction of methane in the fuel mixture is lowered because the flame combustion rate is reduced due to dilution of fuel. In the regime of  $Y_{CH_4} \leq 0.6$ , the envelope flame will transform into a wake one directly when the incoming velocity gradually increases to a limiting value. On the other hand, in the regime of  $Y_{CH_4} > 0.6$ , the lift-off flame, which is only survived for a moment in the experiment, or extinction will appear between the envelope and wake ones as the velocity increases. The possible reason is that the fuel and oxidizer cannot be mixed completely in time and it lacks a recirculation flow to re-ignite the flammable mixture.

After comparing numerical predictions with experimental observed data, the authors believe that the combustion model is suitable to predict the flame transition limits and able to simulate the envelope flames and wake ones. However, for the lift-off flame, this model can only depict an elementary flame structure and phenomenon analyses. It is interesting to investigate the mechanism of lift-off flame toward extinction, since such a phenomenon can result in some safety problems, such as the flights for airplanes and rockets. Hence, the authors continue to develop a transient program to further investigate the detailed transient behaviours. Also, the authors

will continue improving their experiment set-up, such as the addition of PIV and Schlieren system, to measure the flow velocities and temperatures in this flow field. It can further identify the real flame structure except the transition velocity. This would help building a better comparison with the numerical simulations. On the other hand, for numerical simulations, the authors will perform a series of qualitative and quantitative comparisons with experimental observations in the near future. Of course, the multi-step kinetics adopted in the combustion model is also one of the major further investigations. Due to the complexity of combustion and flow, the authors plan to carry out the mention-above works step by step.

## 6 Acknowledgments

The authors would like to thank the National Science Council of the Republic of China for financially supporting this research under Contract No. NSC 92-2212-E-009-013.

## References

- [1] Chen, C.-H. and Weng, F.-B., Flame Stabilization and Blowoff Over a Porous Cylinder, *Combustion Science and Technology*, **73**, 1990, 427-446.
- [2] Jiang, T. L., Chen, W. S., Tsai, M. J., and Chiu, H. H., A Numerical Investigation of Multiple Flame Configurations in Convective Droplet Gasification, *Combustion and Flame*, **103**, 1995, 221-238.
- [3] Tsa, S.S., Chang, C.C., and Chen, C.-H., Experimental Visualizations of Counterflow Diffusion Flame over a Porous Cylinder Burner, Accepted for publication in *Journal of the Chinese Society of Mechanical Engineers*, 2003
- [4] Tsuji, H. and Yamaoka, I., The Counterflow Diffusion Flame in the Forward Stagnation Region of a Porous Cylinder, Eleventh Symposium (International) on Combustion, The Combustion Institute, Pittsburgh, 1967, p. 979.
- [5] Tsuji, H. and Yamaoka, I., The Structure of Counterflow Diffusion Flame in the Stagnation Region of a Porous Cylinder, Twelfth Symposium (International) on Combustion, The Combustion Institute, Pittsburgh, 1969, p. 997.
- [6] Tsuji, H. and Yamaoka, I., Structure Analysis of Counterflow Diffusion Flames in the Forward Stagnation Region of a Porous Cylinder, Thirteenth Symposium (International) on Combustion, 1971, p. 723.
- [7] Tsuji, H., Counterflow Diffusion Flame, *Progress in Energy and Combustion Science*, **8**, 1982, 93.
- [8] Tsuji, H. and Yamaoka, I., Structure Analysis of Anomalous behavior of methane-air and methane-hydrogen-air flames diluted with nitrogen in a stagnation flow, *twenty-fourth Symposium (International) on Combustion*, 1992, pp. 145-152.